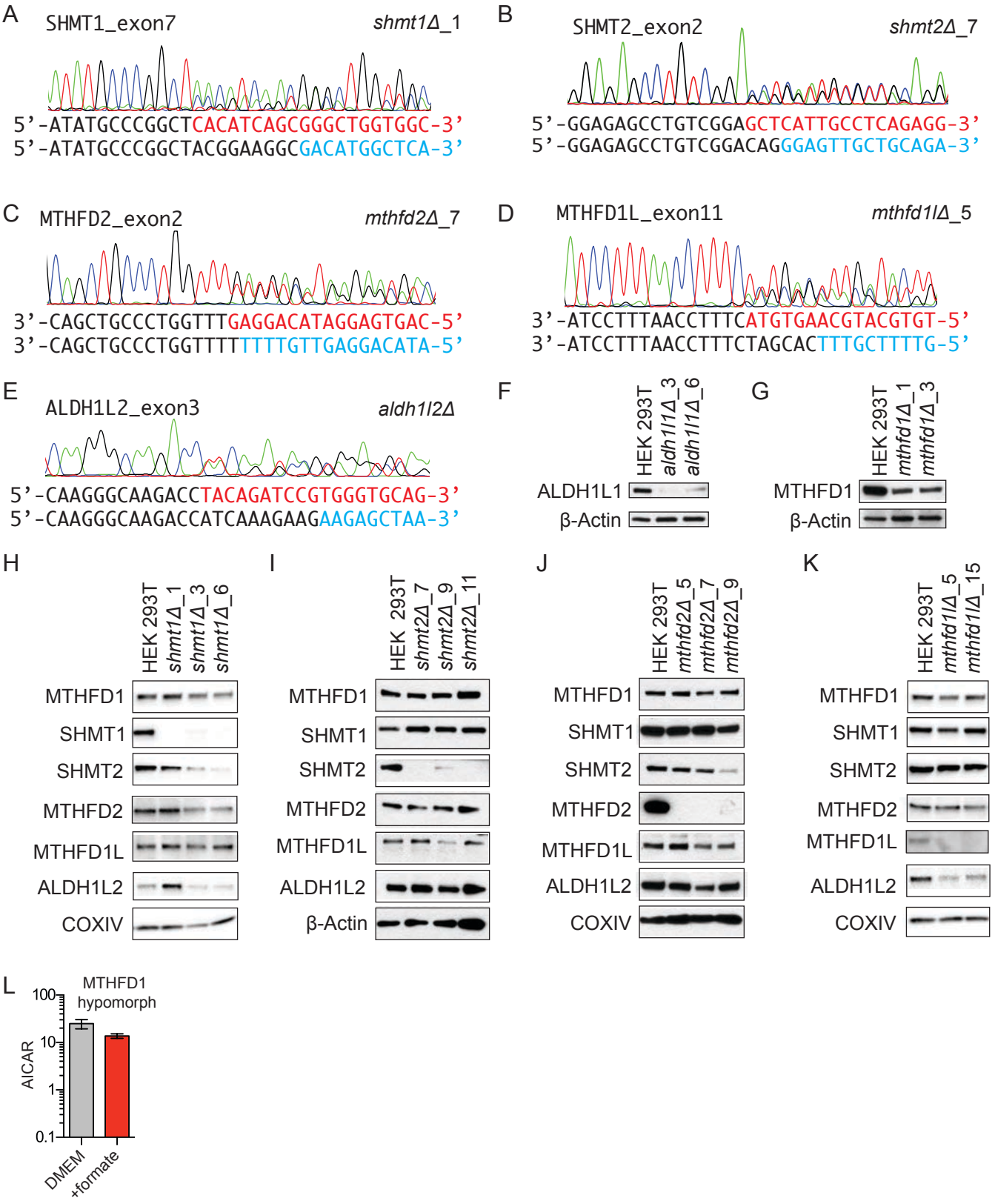

Figure S1: Expression of folate enzymes across multiple independent deletion clones, Related to Figure 1

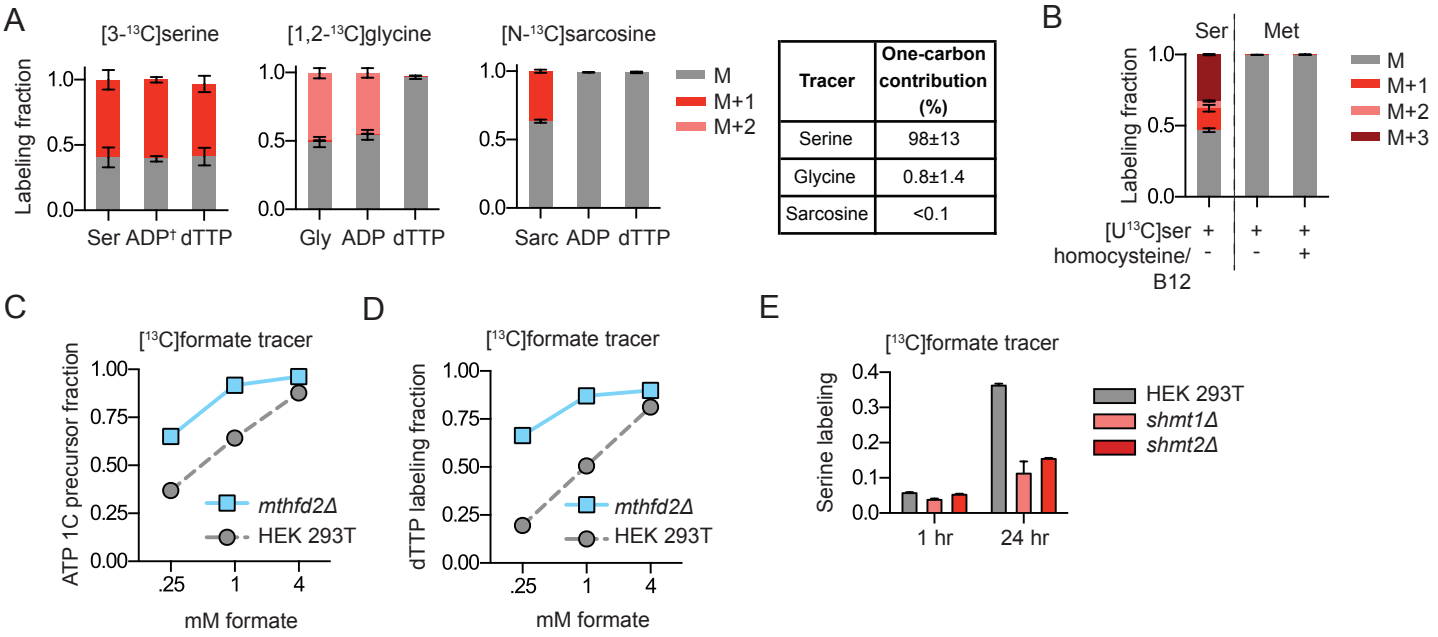

Tracer	One-carbon contribution (%)
Serine	98±13
Glycine	0.8±1.4
Sarcosine	<0.1

Figure S2. 1C units originate from serine or exogenous formate, Related to Figure 2.

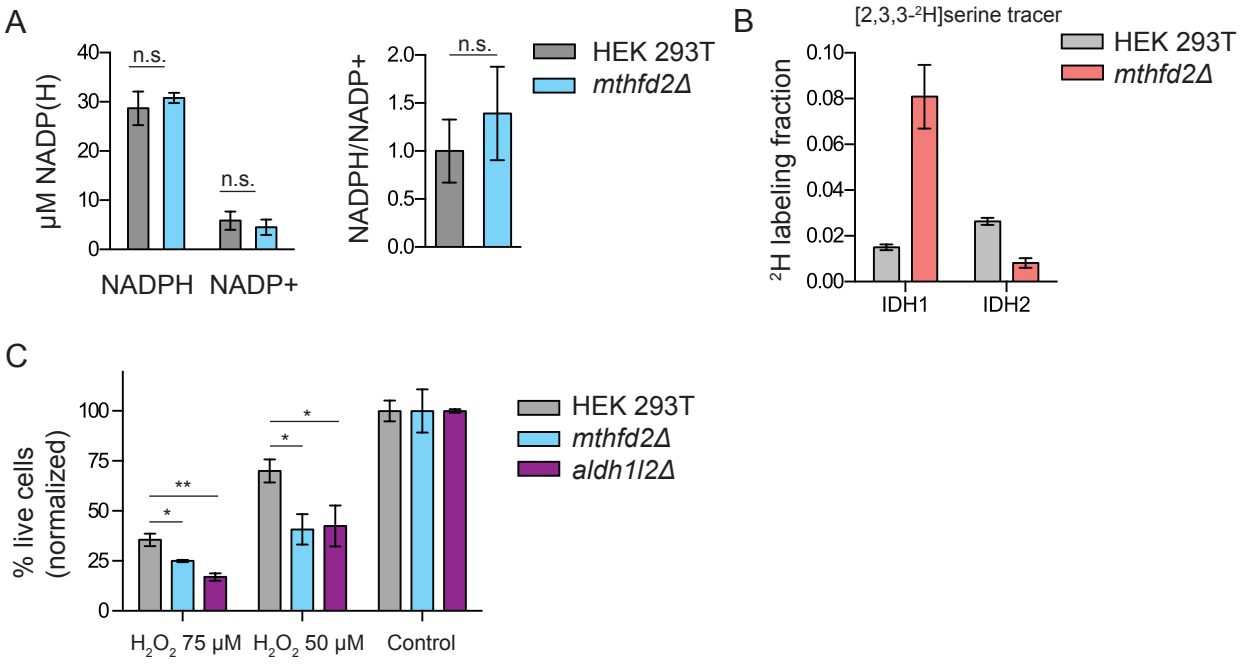

Figure S3: Mitochondrial folate-mediated NADPH production protects cells from oxidative stress, Related to Figure 3

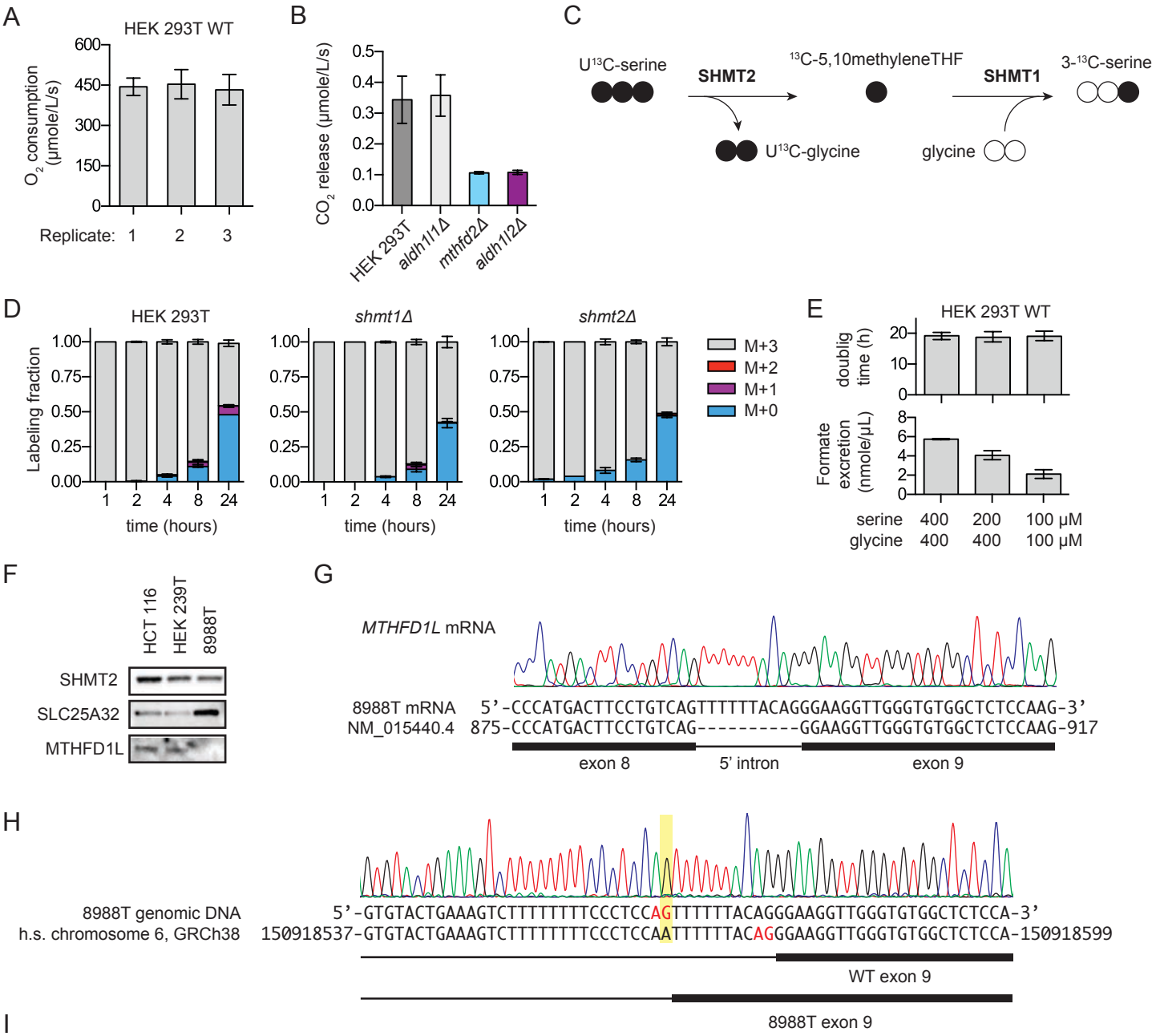

I

Frequency of NG_029185.1(MTHFD1L):g.57888A>G

Population	Allele Count	Allele #	# Homozygotes	Allele Frequency
Latino	1	11576	0	8.64E-05
South Asian	1	16492	0	6.06E-05
European (Non-Finnish)	3	66668	0	4.50E-05
African	0	10406	0	0
East Asian	0	8650	0	0
Other	0	906	0	0
Total	**5**	**121312**	**0**	**4.12E-05**

Figure S4: Mitochondrial folate flux exceeds 1C demand, except in 8988T pancreatic cancer cells that carry a naturally defective *MTHFD1L* allele, Related to Figure 4

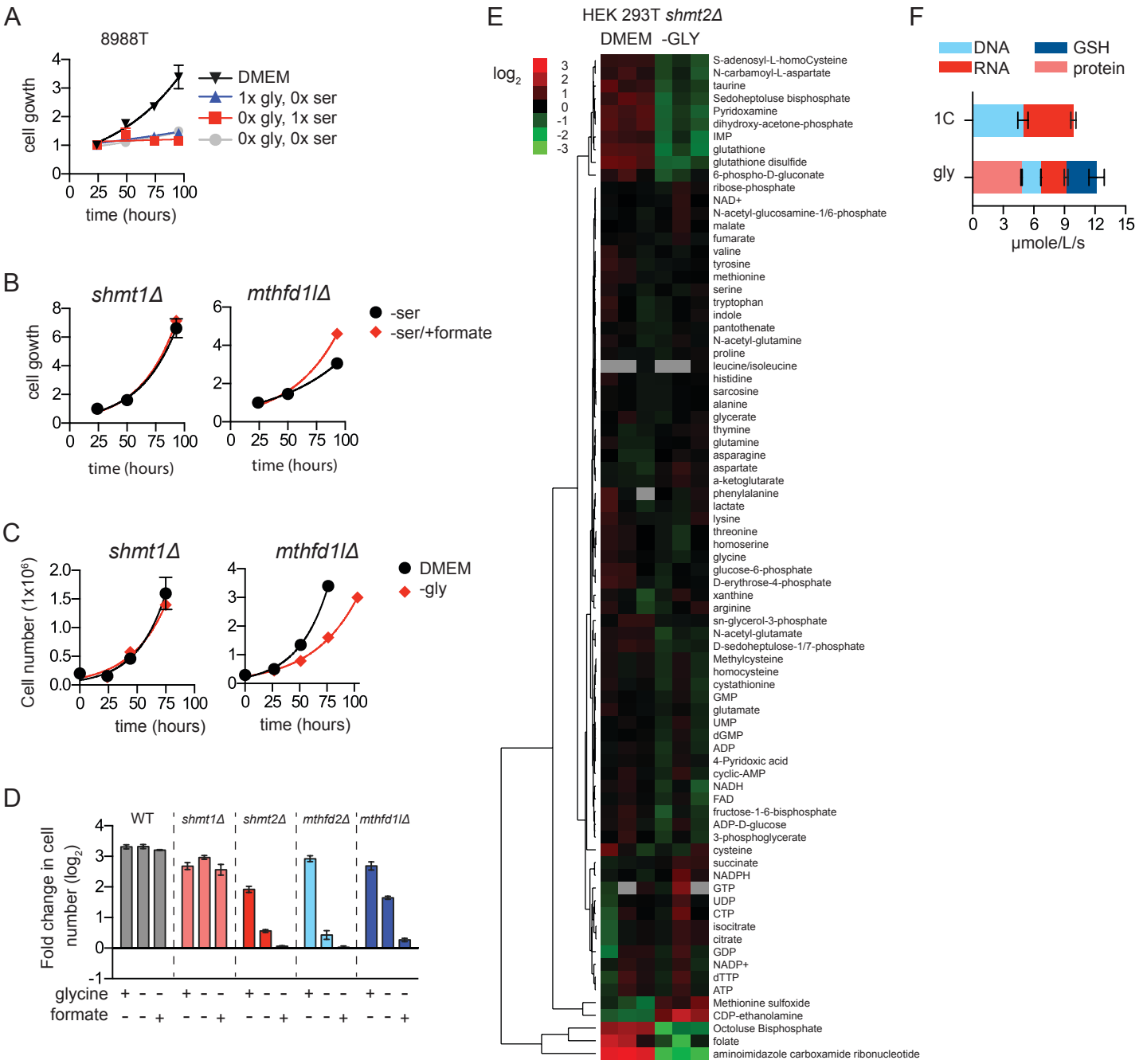

Figure S5: Mitochondrial folate metabolism generates glycine for glutathione, Related to Figure 5

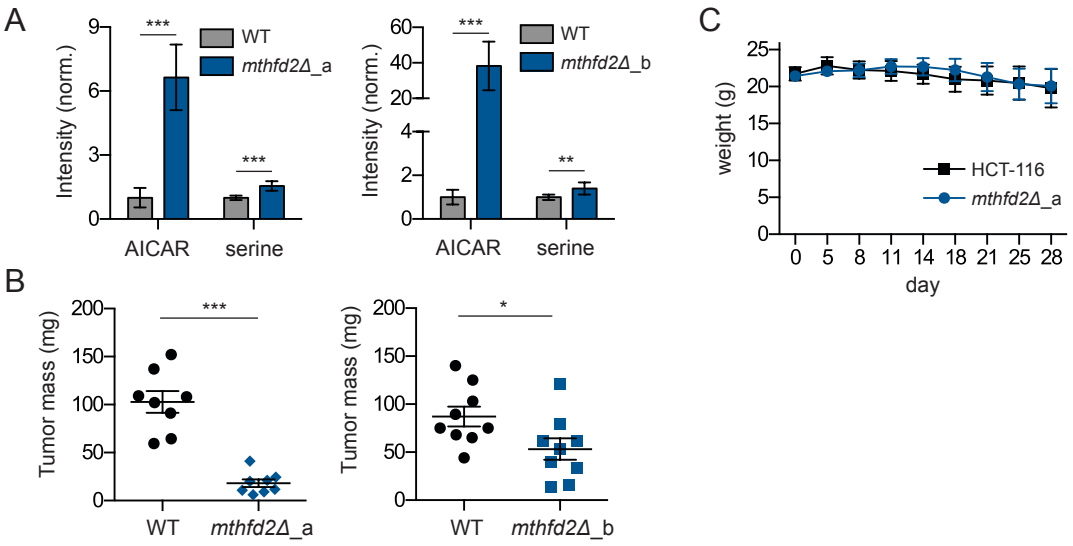

Figure S6: Tumor growth and metabolomics of MTHFD2 deletion clones in NSG mice, Related to Figure 6

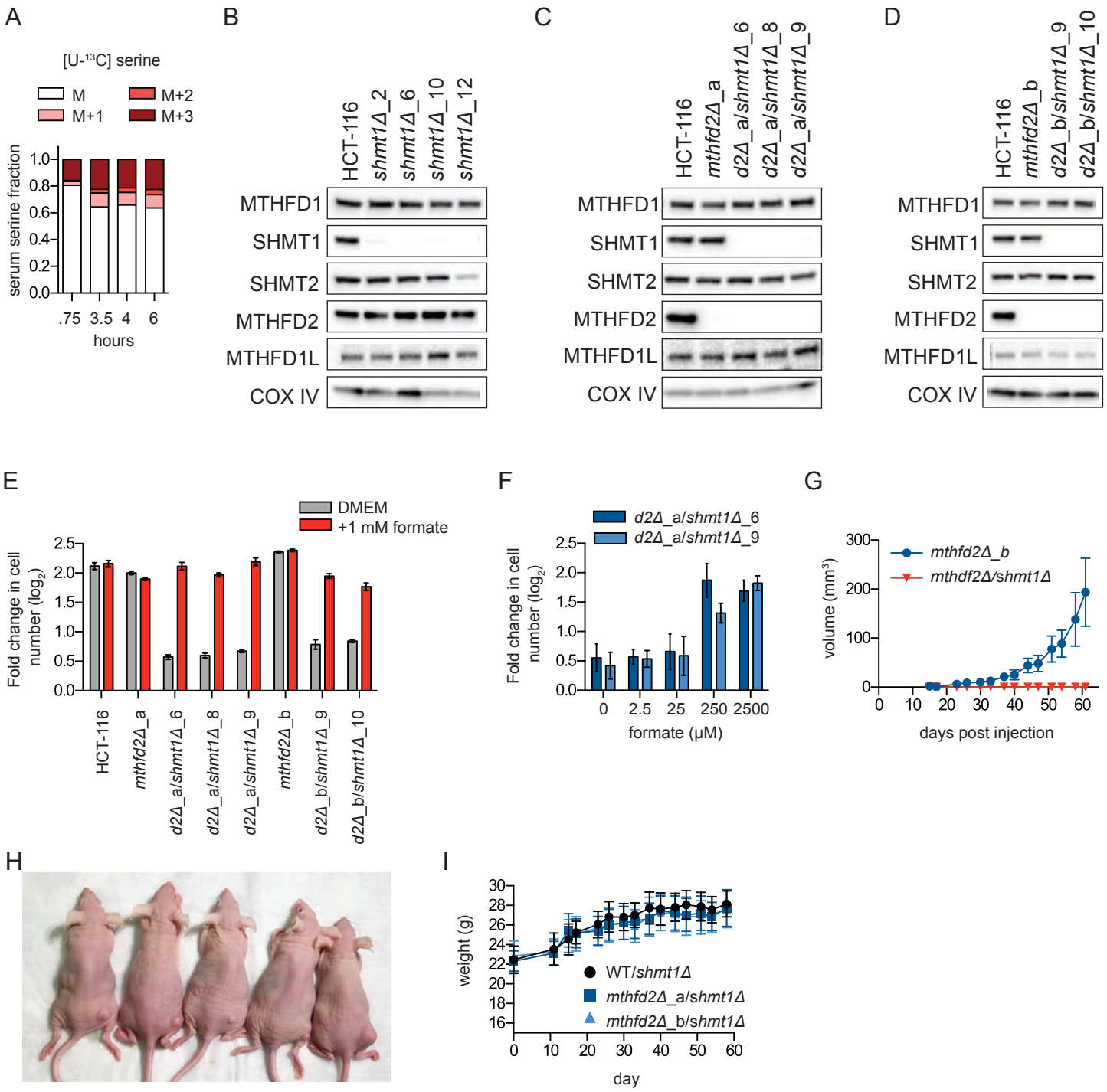

Figure S7: MTHFD2/SHMT1 double mutants are dependent upon formate for growth *in vitro* and fail to form xenografts *in vivo*, Related to Figure 7

Supplemental Figure Legends

Figure S1: Expression of folate enzymes across multiple independent deletion clones, Related to Figure 1. **a-e**. Sanger sequencing of individual deletion clones shows bi-allelic disruption of targeted gene exons. Each genomic sequencing trace shows the point at which the WT (reference human genome) sequence of the CRISPR targeted exon diverges due to an insertion or deletion. WT sequence is shown in black, new sequences shown in red or blue for each copy of the gene. Insertions and deletions were mapped and confirmed to be out of frame. Each sequence trace shown corresponds to a clone used in the main text **f**. Western blot showing expression of ALDH1L1 in two deletion mutants. **g**. Western blot showing reduced expression of MTHFD1 in two hypomorphic cell lines. Each cell line maintains 1 WT copy of the gene. **h-k**. Western blots of deletions clones for SHMT1, SHMT2, MTHFD2 and MTHFD1L showing expression of relevant 1C pathway genes. Clones used in the main text are *shmt1Δ*_1, *shmt2Δ*_7, *mthfd2Δ*_7, *mthfd1l*Δ_5. **l**. AICAR levels (fold-change relative to WT) in MTHFD1 hypomorphic cell lines are not fully rescued by exogenous formate (mean ±SD, n=3).

Figure S2: 1C units originate from serine or exogenous formate, Related to Figure 2.
a. Intracellular metabolite labeling in cells fed labeled ^{13}C-serine, glycine and sarcosine. Total 1C contribution from each precursor calculated by dividing the labeling fraction by the precursor enrichment. ADP labeling reflects 1C precursor labeling fraction†. **b**. Methionine is not labeled by [U-^{13}C]serine in HEK 293T cells, even in presence of added homocysteine and cobalamin (B12). **c**. ATP labeling by [^{13}C]formate. **d**. dTTP labeling by [^{13}C]formate **e**. [^{13}C]formate is incorporated into serine via SHMT1/2. (†) ADP and ATP labeling reflect 1C precursor labeling fraction based on fitting the ADP and ATP mass spectra (after correction for natural isotope abundances) to a binomial (mean ±SD, n≥3).

Figure S3: Mitochondrial folate-mediated NADPH production protects cells from oxidative stress, Related to Figure 3. **a**. Absolute levels of NADP(H) in HEK 293T WT and MTHFD2 deletion cell lines derived by LC-MS using known standards added to ^{13}C-labeled cell extracts. **b**. 2-HG ^{2}H-labeling fraction in HEK 293T WT and *mthfd2Δ* cells incubated with [2,3,3-^{2}H]serine. Mutant IDH1 (cytosolic) and IDH2 (mitochondrial) generate 2-HG in their respective compartments, reporting on localized NADPH. **c**. Total live cells (counted by trypan blue staining and normalized to untreated) after 24 h treatment with indicated concentrations of H_2O_2 (mean ±SD, n≥3, * $p<0.05$; ** $p<0.01$; *** $p<0.001$ by unpaired t-test).

Figure S4: Mitochondrial folate flux exceeds 1C demand, except in 8988T pancreatic cancer cells that carry a naturally defective *MTHFD1L* allele, Related to Figure 4. a. O_2 consumption by HEK 293T cells measured by fluorescence (Seahorse). Results from three independent plates, each with an average of 4 wells. Total NADH production flux is given by O_2 consumption x 0.8 (O_2 for oxidative phosphorylation) x 0.7 (NADH coupled oxphos) x 2 (NADH per O_2) (mean ±SD, n≥4). **b**. CO_2 release from 1C metabolism. Cells were incubated with [3-^{14}C]serine and $^{14}CO_2$ release monitored by scintillation counting (mean ±SD, n≥3). **c**. Schematic showing how [U-^{13}C]serine generates [3-^{13}C]serine by SHMT activity. **d**. Serine isotope scrambling in cells fed [U-^{13}C]serine as measured by LC-MS (mean ±SD, n≥3). **e**. Formate excretion flux depends upon serine concentration. HEK 293T cells were cultured in DMEM with the indicated [3-^{13}C]serine and glycine concentrations for 4 h at which point formate levels were measured by ^{13}C-NMR (mean ±SD, n≥2). Doubling times were unchanged in these media conditions. **f**. Western blot of the mitochondrial folate transporter (SLC25A32) and MTHFD1L in 8988T cells. **g**. Sequencing of reverse transcribed 8988T *MTHFD1L* mRNA shows an insertion between exons 8 and 9 compared to the human reference sequence transcript (NM_015440.4). The 10 bp insertion in the 8988T mRNA matches the intronic sequence immediately 5' of exon 9. **h**. Genomic sequencing of 8988T DNA shows a point mutation (A>G, highlighted in yellow) that creates a *de novo* splice site 5' to the canonical site (highlighted in red). **i**. Allele frequency for the identified *MTHFD1L* splicing mutant variant from the ExAC (Exome Aggregation Consortium, http://exac.broadinstitute.org/) database.

Figure S5: Mitochondrial folate metabolism generates glycine for glutathione, Related to Figure 5. a. 8898T pancreatic cancer cells naturally defective in MTHFD1L depend on exogenous serine and glycine to grow. 8988T cells were cultured for 4 days in DMEM with and without serine and glycine. **b.** Growth in serine free media is attenuated in MTHFD1L, but not SHMT1, deletion HEK 293T cell lines. 1 mM formate rescues growth in MTHFD1L deletion cells. **c**. Growth in glycine free media is attenuated in MTHFD1L, but not SHMT1, deletion cell lines. **d**. In glycine free media, 1 mM formate worsens growth of mitochondrial folate deletion cell lines, but not WT or SHMT1 deletion cell lines. Growth is plotted as $\log_2$ of the total fold change in cells in a 4 day experiment. (mean ±SD, n≥3) **e**. A heat-map showing changes in metabolite abundances between *shmt2Δ* cells cultured in DMEM with and without glycine. Each metabolite was row normalized using $\log_2$ of the measured abundance. **f**. Calculated demand for 1C units and glycine in dividing HEK 293T cells.

Figure S6: Tumor growth and metabolomics of MTHFD2 deletion clones in NSG mice, Related to Figure 6. a. AICAR and serine levels from HCT-116 WT and MTHFD2 deletion xenografts. Metabolite intensities are from LC-MS and reported as fold changes compared to WT tumors (mean ±SD, n=6, $p<0.05$; ** $p<0.01$; *** $p<0.001$ by unpaired t-test). **b.** The final tumor masses (mean ±SD, n≥8,). **c**. Weights of nude mice bearing tumors from Figure **6k**.

Figure S7: MTHFD2/SHMT1 double mutants are dependent upon formate for growth *in vitro* and fail to form xenografts *in vivo*, Related to Figure 7. a. Serum serine labeling upon constant infusion with 200 mM [U-^{13}C]serine. Tail vein blood draws were serially performed at the indicated time post start of infusion. Serine isotope enrichment was quantified by LC-MS (from a single mouse). **b**. Western blot showing missing SHMT1 protein expression in *shmt1Δ* cell lines isolated from single colonies using CRISPR. **c-d**. Western blot showing missing SHMT1 protein expression in *mthfd2Δ*_a/*shmt1Δ* and *mthfd2Δ*_b/*shmt1Δ* cell lines isolated from single colonies using CRISPR and selected in media containing 1 mM formate. **e**. Cell growth of *mthfd2Δ*/*shmt1Δ* double deletion cell lines ±1 mM formate. Growth is plotted as $\log_2$ of the total fold change in cells in a 2-day experiment **f**. Effect of extracellular formate concentration on cell growth in *mthfd2Δ*/*shmt1Δ* double deletion cell lines. Growth is plotted as $\log_2$ of the total fold change in cells in a 2-day experiment. **g**. Tumor volumes of *mthfd2Δ*_b/*shmt1Δ* and *mthfd2Δ* _b cells grown as bilateral xenografts on nude mice. Tumor volumes calculated from caliper measurements biweekly (Methods) (mean ±SEM, n=8). **h**. Representative mice from (**g**) 8 weeks post injection with *mthfd2Δ* (right) and *mthfd2Δ/shmt1Δ* (left) cells. **i**. Weights of tumor bearing mice (nude) from the *shmt1Δ* and *shmt1Δ/mthdf2Δ* double deletion xenograft experiments in figures **7f,h** and (**g**) (mean ±SEM, n≥8).

Table S1, related to Experimental Procedures

Gene	Exon	Targeting Sequence	Fwd Primer	Rev Primer
SHMT1	7_fwd	GGCGTATCTCATGGCGGACA**TGG**	CACCGGCGTATCTCATGGCGGACA	AAACTGTCCGCCATGAGATACGCC
SHMT1	7_rev	CATCTGCAATCTTCCGTAGC**CGG**	CACCGCATCTGCAATCTTCCGTAGC	AAACGCTACGGAAGATTGCAGATGC
SHMT2	2_fwd	GGACAGGCAGTGTCGTGGCC**TGG**	CACCGGACAGGCAGTGTCGTGGCC	AAACGGCCACGACACTGCCTGTCC
SHMT2	2_rev	TCTCAGGATCACTGTCCGAC**AGG**	CACCGTCTCAGGATCACTGTCCGAC	AAACGTCGGACAGTGATCCTGAGAC
MTHFD2	2_fwd	CGCCAACCAGGATCACACTC**AGG**	CACCGCGCCAACCAGGATCACACTC	AAACGAGTGTGATCCTGGTTGGCGC
MTHFD2	2_rev	CTATGTCCTCAACAAAACCA**GGG**	CACCGCTATGTCCTCAACAAAACCA	AAACTGGTTTTGTTGAGGACATAGC
MTHFD1L	11_fwd	GGAAAATACGTCTTAGTTGC**TGG**	CACCGGAAAATACGTCTTAGTTGC	AAACGCAACTAAGACGTATTTTCC
MTHFD1L	11_rev	TAGCACGGACAAACGTACTT**TGG**	CACCGTAGCACGGACAAACGTACTT	AAACAAGTACGTTTGTCCGTGCTAC
ALDH1L1	3_fwd	TAGATGATGGAGCCATGCCG**GGG**	CACCGTAGATGATGGAGCCATGCCG	AAACCGGCATGGCTCCATCATCTAC
ALDH1L1	3_rev	ACTGCTCCCTAGGCACCGAG**GGG**	CACCGACTGCTCCCTAGGCACCGAG	AAACCTCGGTGCCTAGGGAGCAGTC
ALDH1L2	3_fwd	GCAGAAGCCTACAGATCCGT**GGG**	CACCGCAGAAGCCTACAGATCCGT	AAACACGGATCTGTAGGCTTCTGC
ALDH1L2	3_rev	TTGCCCTTGACCCTCCATTT**AGG**	CACCGTTGCCCTTGACCCTCCATTT	AAACAAATGGAGGGTCAAGGGCAAC
MTHFD1	1_fwd	AGGGAGTGGAACCTCGATAT**TGG**	CACCGAGGGAGTGGAACCTCGATAT	AAACATATCGAGGTTCCACTCCCTC
MTHFD1	1_rev	ACAACCCAACCCACGTGCTT**AGG**	CACCGACAACCCAACCCACGTGCTT	AAACAAGCACGTGGGTTGGGTTGTC
NNT	2_fwd	GACCCCAAATTGCTAAGTAG**AGG**	CACCGACCCCAAATTGCTAAGTAG	AAACTACTTAGCAATTTGGGGTC
NNT	2_rev	TAAGGGTCTACGTGTGAAGA**AGG**	CACCGTAAGGGTCTACGTGTGAAGA	AAACTCTTCACACGTAGACCCTTAC

Table S1: CRISPR primers. Gene name, targeting sequences and primers used to generate knockout cell lines used in this study.

Supplemental Experimental Procedures

Cell lines, reagents, constructs and antibodies

Fresh aliquots of HEK 293T/17 (CRL-11268, lot# 60840695) and HCT-116 (CCL-247, lot# 60506215) were purchased from ATCC (Manassas, VA) before beginning experiments. MDA-MB-468, MDA-MB-231, BT-20, HeLa, MCF7, 3T3-L1, Jurkat, A549, LNCaP and LN229 cells were from ATCC; 8988T and 8988S cell were from DSMZ (Braunschweig, Germany); Kelly cells were provided by Craig Thompson (Memorial Sloan Kettering Cancer Center); iBMK cells were provided by Eileen White (Rutgers) (Degenhardt et al., 2002); human foreskin fibroblasts (HFF) were provided by Thomas Shenk (Princeton University). Cell lines were subcultured in 5% CO_2 at 37°C using DMEM (CellGro 10-017, Mediatech Inc., Manassas, VA) supplemented with 10% fetal bovine serum (F2442, Sigma-Aldrich, St. Louis, MO) except for Jurkat and LNCaP cells which were cultured in RPMI-1640 (CellGro 10-040) with 10% serum. For all experiments, media supplemented with 10% dialyzed fetal bovine serum was used (F0392, Sigma-Aldrich). Cas9 nickase and guide RNA expression plasmid pSpCasn(BB)-2A-Puro (48141) was purchased from Addgene (Cambridge, MA). All primers were synthesized by IDT (Coralville, IA). Antibodies were used according to their manufacturer's directions. Anti-SHMT1 (12612), SHMT2 (12762), β-actin (5125), COXIV (4850), ACC (3662), p-ACC (S79) (3661), AMPK (5831), p-AMPK (T172) (2535) were obtained from Cell Signaling Technologies (Danvers, MA). Anti-MTHFD1L (ab153840), ALDH1L1 (ab175198), ALDH1L2 (ab113496), SLC25A32 (ab62192), MTHFD2 (ab151447) and MTHFD1 (ab70203) were obtained from Abcam Inc. (Cambridge, MA).

Isotopic labeling

Isotopic tracers were purchased from the following sources: [2,3,3-^{2}H]serine, [3-^{13}C]serine, [U-^{13}C]serine, [U-^{13}C]glycine, [^{2}H-^{13}C]formate (Cambridge Isotope Laboratories, Cambridge MA); [^{13}C]formate (Sigma-Aldrich); [3-^{14}C]serine (American Radiolabeled Chemicals, St. Louis, MO). Serine and glycine isotopically labeled media was prepared from scratch as described using dialyzed FBS. Formate (0.25, 1 or 4 mM) was added to complete DMEM.

Immunoblotting

1x10^{6} cells were cultured in each well of a 6-well plate. Media was removed and cells rinsed once with 4°C PBS and lysed in radio-immunoprecipitation assay (RIPA) buffer with added phosphatase and protease inhibitors (Roche, Indianapolis IN). Lysates were cleared by 10 min centrifugation at 16,000 x g, and equilibrated to 2 mg/mL after protein quantification using a BCA assay in 96-well format (Pierce). Samples were resolved by sodium dodecyl sulfate–polyacrylamide gel electrophoresis on 4-20% gradient gels (Bio-Rad, Hercules, CA) and transferred to nitrocellulose. After overnight incubation with primary antibodies, bands were visualized with horseradish peroxidase-conjugated secondary antibodies and chemiluminescence (Pierce) using x-ray film.

NMR detection of formate in cultured cells

Formate production was measured by changing the culture medium on cells growing in 10 cm dishes (50-70% confluent) to contain [3-^{13}C]serine (400 μM), and media was collected at 2, 4, 8 and 24 hours. For each measurement, 5 mL media was collected from cells, and spiked with 1 μmol of [^{2}H-^{13}C]formate, before precipitation with 5 mL of acetonitrile. The supernatant was dried down under nitrogen flow and resuspended in 500 μL D_2O. Samples were run on a Bruker 500MHz NMR equipped with a DCH cryoprobe optimized for ^{13}C observation, and 512 scans were collected for each sample. Data was analyzed using MNova 9.0 software. [^{2}H-^{13}C]formate showed triplet peaks at 171.33, 171.09 and 170.85 ppm and [^{1}H-^{13}C]formate at 171.24 ppm. Quantification of [^{1}H-^{13}C]formate was achieved by calculating the ratio of peak area of [^{1}H-^{13}C]formate over [^{2}H-^{13}C]formate, which was added in known concentration. The rate of formate production from serine was calculated by solving the following equation for R_f (formate production rate):

$$\frac{d[^{13}\text{C]Formate}}{dt} = R_f(1 - Se^{at})C_0e^{kt} \quad (2)$$

where t= time (hrs), C_0 = PCV (Packed cell volume) at time 0 in μL, S, and a are best fit values obtained from fitting the ^{13}C-serine unlabeled fraction to an exponential, and k is $\ln_2$/(doubling time).

Folate measurements

To isolate folate species, growth media from DMEM cultured cells was aspirated and replaced with freshly prepared ice-cold lysis buffer (1:1 methanol: water, 0.5% w/v sodium ascorbate and 0.3% w/v NH_4OAc; pH 7.0). Cellular debris was scrapped from culture plates, centrifuged at 5,000 x g and the supernatants collected. Samples were dried under N_2 flow before resuspension in buffer (25 mM $K_2PO_4H_2$, 0.5% sodium ascorbate, 0.5% BME; pH=7.0) and treated with rat serum

(Sigma) for 2 h at 37°C. Samples were acidified to pH 4 with formic acid before loading on conditioned (1 mL methanol, 1 mL wash buffer) Bond Elute-Ph SPE columns (Agilent). Samples were washed once with 1 mL wash buffer (0.5 % ascorbic acid in 0.3% NH_4OAc buffer at pH=4). Folate species were eluted in 400 μL methanol buffer (1:1 Methanol: water, 0.5% BME, 0.3% NH_4OAc; pH 7.0). Samples were dried down and resuspended in pure water before analysis on an orbitrap mass spectrometer (ThermoScientific Exactive) operating in negative ion mode coupled to a reverse phase ion-pairing HPLC as described previously (Lu et al., 2010). Known folate standards were used to confirm the identity of all species.

Flux measurements

For all experiments, flux measurements are reported in units of μmol/L/s (equivalent to pmol/μL/s). For HEK 293T cells, the reported flux values (pmol/μL/s) can be converted to units of cell number (pmol/($1x10^6$ cells)/s) by multiplying by 2.5 ($4x10^5$ HEK 293T cells/ μL). This can be further converted to a flux of molecules per cell ($1x10^5$ molecules/cell/s) by dividing by 6.02. To instead normalize by mg of cellular protein (pmol/mg(protein)/s), multiply reported flux values by 7.1 (0.14 mg protein/μL for HEK 293T cells). Values for these conversions were constant among the different HEK 293T mutant cell lines.

CO_2 release from serine

$^{14}CO_2$ production was quantified as previously described (Fan et al., 2014). Briefly, cells were grown in 12.5 cm^2 tissue culture flasks with DMEM with low bicarbonate (0.74 g/L) and additional HEPES (6g/L, pH 7.4). 3-^{14}C serine (98 μCi/mL final) was added to the media (3 mL) and the flask was sealed with a stopper with a center well (Kimble Chase) containing thick pieces of filter paper saturated with 100 μL 10 M KOH. Cells were incubated for 24 h. Reactions were quenched with 1 mL 3M acetic acid. Filter paper (and any associated residue) in the center well was collected into liquid scintillation cocktail (Ultima Gold, PerkinElmer, Waltham, MA). The signal was corrected for intracellular substrate labeling according to percentage of radioactive tracer in the media, and fraction of particular intracellular metabolite from media uptake, which was measured by ^{13}C-tracer. The ^{14}C flux (per packed cell volume per hour) is given by:

$$^{14}CO_2 = \frac{^{14}\text{C signal}}{\text{Labeling time} \times \text{PCV}} \times \frac{^{12}\text{C substrate}}{^{14}\text{C tracer}} \times \frac{\text{Fraction medium nutrient } ^{13}\text{C labeled}}{\text{Fraction intracellular substrate } ^{13}\text{C labeled}} \qquad (3)$$

1C and glycine carbon contribution to biosynthesis

Demand for 1C and glycine units for RNA and DNA was calculated using total RNA and DNA values for HEK 293T cells and experimentally derived growth rates (Fan et al., 2014). Total 1C demand for DNA and RNA was calculated to be 7.2 μmol/L/s each and glycine demand for RNA and DNA to be 2.9 and 3.6 μmol/L/s for DNA and RNA respectively. *De novo* serine synthesis consumption of 1C units was calculated from the serine scrambling assay shown in Figure S4d. The rate of serine re-synthesis was calculated by converting the M+1 labeling fraction into absolute concentration and using linear regression to calculate the production rate per hour. Total glutathione demand was calculated from direct measurement of cellular glutathione concentrations (total pool of reduced plus oxidized of 9.6 mM) and quantification of glutathione turnover using isotope tracing ($t_{1/2}$ = 4 hrs).

Transcript sequencing

Total cellular RNA was extracted using the RNeasy mini extraction kit (Qiagen, Germantown, MD). Select mRNAs were reverse transcribed and amplified using transcript specific primers and the OneTaq RT-PCR kit (E5315S, New England Biolabs, Ipswich, MA). Gene specific primers used (FWD/REV): *SHMT1* (CCAGTGCAATGACGATGCCAG/ AGCAGCTCATCCATCTCTCAG), *SHMT2* (CGTAGATCCCTCCCGTTAGC/ GCCAGACGCTGA CTTGTTTC), *MTHFD1* (ACGTGGGTTGGG TTGTCCTG / GGGCTGACTTCTCTTGGCTTAC), *MTHFD2* (CACGAGGCCGCAGTATAACC / TTGGCCTGCTTTGCTTCTTG), *SLC25A32* (TAAGAGTCCTCTCGTTGGTCC / AAGAGCTTGTT GCTGCCTTGG), *MTHFD1L* (GCCTTCAA GCCGGTTCTTGC / AGTTATTGGCAGCGGTGA TGG).Transcripts were sequenced by Sanger sequencing.

Natural abundance, KIE and NADPH calculations

Carbon isotope labeling patterns were corrected for ^{13}C natural abundance. Whenever possible, based upon our Orbitrap mass resolution of 100,000 at 200 Da, ^{2}H peaks were separated from other isotopes by the mass spectrometer. When ^{2}H peaks were not directly resolvable, they were corrected for ^{13}C, ^{18}O, and ^{15}N natural abundance (correction was only required for the unresolvable combination of 1 or 2 ^{13}C, ^{18}0 and ^{15}N atoms). Correction was done by least squares (NNLS package in R) solving for the deuterium labeling vector, [D_0, D_1, …, D_i,…. D_n], where n = the number of hydrogens in the molecule, and D_i is ^{2}H labeling fraction for deuterium i, using the following equation:

$$\begin{bmatrix} (0,x_c,N_c) & 0 & 0 & 0 & \dots & 0 \\ (1,x_c,N_c) & (0,x_c,N_c) & 0 & 0 & \dots & 0 \\ (2,x_c,N_c) & (1,x_c,N_c) & (0,x_c,N_c) & 0 & \dots & 0 \\ 0 & (2,x_c,N_c) & (1,x_c,N_c) & (0,x_c,N_c) & \dots & 0 \\ \dots & \dots & \dots & \dots & \dots & \dots \\ 0 & 0 & 0 & 0 & \dots & (0,x_c,N_c) \end{bmatrix} \times \begin{bmatrix} {}^{18}O \\ correction \end{bmatrix} \times \begin{bmatrix} {}^{15}N \\ correction \end{bmatrix} \times \begin{bmatrix} D_0 \\ D_1 \\ \dots \\ D_i \\ \dots \\ D_n \end{bmatrix} = \begin{bmatrix} M \\ M+1 \\ \dots \\ M+i \\ \dots \\ M+n \end{bmatrix} \quad (4)$$

$$(i,x_c,N_c) = \binom{x_c}{i}(1-N_c)^{x_c-i}(N_c)^i \quad (5)$$

x_c is the number of carbon atoms, N_c is the natural abundance of ^{13}C, and [*M, M+1, ..., M+i, ..., M+n*] is the measured isotopic labeling distribution vector. ^{18}O and ^{15}N correction matrices follow the same formula (with ^{18}0 and ^{15}N natural abundances substituting for N_c, and O and N atom numbers x_O and x_N substituting for x_c respectively).

To determine the labeling percentage of NADPH from palmitate, the natural abundance corrected ^{2}H isotopic distribution was fit to a binomial distribution using least squares in Matlab. The calculated labeling fraction (x) was then adjusted for the KIE of fatty acid synthase (V_H/V_D = 1.1, (Yuan and Hammes, 1985)) using the following equation:

$$NADPH_{adj} = \frac{\frac{x}{1-x}}{\frac{1}{\frac{V_H}{V_D}} + \frac{x}{1-x}} \quad (6)$$

The net impact of this correction was to adjust the calculated labeling fraction by ~9%. This adjusted value gives the cellular NADPH labeling fraction. We then further corrected for the KIE of the enzyme making NADPH and the fraction of substrate labeling. The KIE for making NADPH was conservatively corrected with the following equation which assumes no change in pathway flux (Fan et al., 2014).

$$C_{KIE} = \frac{V_H}{V_D} + x\left(1 - \frac{V_H}{V_D}\right) \quad (7)$$

where x is the observed fraction labeling of relevant hydrogen, V_H/V_D is the measured kinetic isotope effect and C_{KIE} is the corrected labeling fraction. A measured ^{2}H-KIE of 2.87 was used for NADPH synthesis from MTHFD2 and MTHFD1 (Schmidt et al., 2000), adjusting the labeling fraction by approximately 45%. After KIE correction, NADPH labeling was finally corrected for intracellular substrate labeling (serine M+3 and M+2 fraction) to obtain a final calculated contribution of serine to NADPH production. Malate labeling was KIE and substrate labeling corrected following equation 5 and same ^{2}H-KIE for MTHFD2 to obtain the calculated NADH production from serine.

Formate measurements from mouse serum

Formate in mouse serum was quantified using pentafluorobenzyl bromide (PFBBr) derivatization followed by detection using gas chromatography mass spectrometry (GC-MS) (Lamarre et al., 2014). From a terminal cardiac draw, 25 µL of cleared serum dissolved in phosphate buffer (pH 8.0) containing a [^{2}H-^{13}C]formate internal standard was treated with 100 mM PFBBr in acetone and heated to reflux for 15 minutes. The mixture was concentrated by 50% under nitrogen stream prior to being extracted with hexanes. Samples were run on an Agilent 5975C inert XL EI/CI MSD mass spectrometer with monitoring for the following masses corresponding to PFBBr derivatized formate with and without isotope labeling (m/z= 226, 227, 228).

Supplemental References

Degenhardt, K., Chen, G., Lindsten, T., and White, E. (2002). BAX and BAK mediate p53-independent suppression of tumorigenesis. Cancer Cell *2*, 193–203.

Fan, J., Ye, J., Kamphorst, J.J., Shlomi, T., Thompson, C.B., and Rabinowitz, J.D. (2014). Quantitative flux analysis reveals folate-dependent NADPH production. Nature *510*, 298–302.

Lamarre, S.G., MacMillan, L., Morrow, G.P., Randell, E., Pongnopparat, T., Brosnan, M.E., and Brosnan, J.T. (2014). An isotope-dilution, GC–MS assay for formate and its application to human and animal metabolism. Amino Acids *46*, 1885–1891.

Lu, W., Clasquin, M.F., Melamud, E., Amador-Noguez, D., Caudy, A.A., and Rabinowitz, J.D. (2010). Metabolomic

Analysis via Reversed-Phase Ion-Pairing Liquid Chromatography Coupled to a Stand Alone Orbitrap Mass Spectrometer. Anal. Chem. *82*, 3212–3221.

Schmidt, A., Wu, H., MacKenzie, R.E., Chen, V.J., Bewly, J.R., Ray, J.E., Toth, J.E., and Cygler, M. (2000). Structures of Three Inhibitor Complexes Provide Insight into the Reaction Mechanism of the Human Methylenetetrahydrofolate Dehydrogenase/Cyclohydrolase. Biochemistry *39*, 6325–6335.

Yuan, Z.Y., and Hammes, G.G. (1985). Elementary steps in the reaction mechanism of chicken liver fatty acid synthase. Acylation of specific binding sites. J Biol Chem *260*, 13532–13538.